

This is the peer reviewed version of the following article:

Single-arm Self-mixing Superluminescent Diode Interferometer for Flow Measurements / Di Cecilia, Luca; Cattini, Stefano; Giovanardi, Fabio; Rovati, Luigi. - In: JOURNAL OF LIGHTWAVE TECHNOLOGY. - ISSN 0733-8724. - 35:16(2017), pp. 3577-3583. [10.1109/JLT.2016.2583919]

Terms of use:

The terms and conditions for the reuse of this version of the manuscript are specified in the publishing policy. For all terms of use and more information see the publisher's website.

11/01/2026 18:02

Single-arm Self-mixing Superluminescent Diode Interferometer for Flow Measurements

L. Di Cecilia, S. Cattini, *Member, IEEE*, F. Giovanardi, and L. Rovati, *Member, IEEE*

Abstract—Laser-diode self-mixing interferometry is a noncontact technique widely used both in industries and laboratories. In this paper we propose to extend the self-mixing approach to low-coherence sources such as superluminescent diodes. In particular, we present a fiber-based common-path interferometer exploiting a single mode pigtailed super-luminescent diode. The developed measuring system has been demonstrated to be able to directly measure the flow in pipes. To the best of our knowledge, it is the first time that flow measurements have been performed by a single-arm self-mixing pigtailed super-luminescent-diode. The measuring system exploits the Doppler interference pattern produced by the light back-reflected from the inner facet of the pipe wall and the light back-diffused by the moving particles. Then, the use of a low-coherence source allows to measure the velocity of the scattering particles in a fixed and well defined region located close to the pipe wall, thus providing good robustness to variations of scatterers concentration and allowing to easily estimate the flow under the laminar flow assumption. Experimental results demonstrated a high linearity (Pearson coefficient of about 99%) and sensitivity of about $16.62 \pm 1.1 \text{ cm}^{-3}$, with flows ranging from $1 \text{ cm}^3/\text{s}$ to $15 \text{ cm}^3/\text{s}$ and scatterers volume concentration ranging from 0.015% to 0.36%.

Index Terms—optical velocity measurement, flow measurement, optical interferometry, low-coherence interferometry, optical feedback.

I. INTRODUCTION

THE laser-diode (LD) self-mixing (SM) (or feedback) interferometry is a noncontact method widely used both in industrial and laboratory applications to measure quantities such as velocity (of both solid targets and fluids), displacement, vibration and distance [1–3]. In SM systems, no external photodetector is required, because the signal is directly analyzed by the back facet monitor photodiode (MPD) usually contained in the LD package. Moreover, the same optic acts as both illumination and collection optics, allowing to obtain a much simpler and robust system and lower associated costs. Furthermore, to reach the back facet monitor photodiode the detected fields have to retrace back the active region of the used light source, thus the sensitivity of the scheme is improved by the amplification provided by the active region itself. Nevertheless, despite great progress in the development of SM-LD interferometer based technologies, there remains significant interest in further development of applying the same approach in low-coherence sources like superluminescent diodes.

The authors are with the Department of Engineering "Enzo Ferrari", University of Modena and Reggio Emilia, Via Vivarelli 10, Modena, Italy. S. Cattini, and, L. Rovati are also with the Science & Technology Park for Medicine, TPM, Democenter Foundation Mirandola, Modena, Italy (e-mail: luca.dicecilia@unimore.it).

Manuscript received XXX; accepted XXXX.

Indeed, the common-path setup exploited in SM-LD can be applied also with super-luminescent-diode (SLD) sources if at least two external cavities are present [4]. In such simple optical design, the sample and reference arms share a common path. A common-path interferometer based on a SLD and exploiting a free space interferometer multiple paths has been reported [4].

In recent years we have been exploiting SM effect in the SLD cavities to measure the fluid-velocity profile in pipes [5]. In this paper we present for the first time a fiber-based interferometer to measure directly the flow in a pipe based on a single-arm approach. The system exploits the SM effect in a single mode pigtailed super-luminescent diode. The interferometer recovers from the Doppler signal the velocity of the scattering particles flowing in a fixed and well defined region located close to the pipe wall and, under the laminar flow assumption, it provides a first estimation of the flow-rate.

The article is divided in four parts. In section II we present the measuring principle and outline its main features. The developed measuring system and the performed experimental activities are described in the section III. Then, preliminary measurements demonstrating the applicability of the proposed measurement system are reported in section IV and discussed in section V.

II. THEORETICAL MODEL

The primary objective of this section is to describe the fundamental concepts and the theoretical model of the optical feedback interferometry in a super-luminescent diode and its application in recovering the velocity of scattering particles in a laminar flow exploiting the Doppler signal.

A. Self-mixing effect in a superluminescent diode

Superluminescent diodes are known to be non-monochromatic sources. Like laser diodes (LD), SLDs have a monitor photodiode placed in the same case of the optical source on the emitting junction backface. As in self-mixing laser diode (SMLD) interferometry, this photodiode is used to detect the variation of the emitted optical power induced by any light back-reflected back to the superluminescent diode. A conceptual optical scheme describing the SLD optical feedback in our setup is shown in Fig.1. In the figure two semitransparent flat surfaces define the section of an ideal pipe containing flowing particles. The light from the SLD, collimated by the lens L, illuminates the two surfaces S_1 and S_2 and the particles flowing in the pipe.

The surfaces and particles act as several external cavities where the light is more or less confined depending

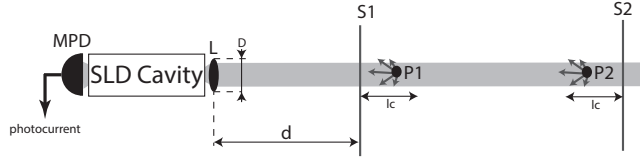


Fig. 1. Conceptual optical scheme describing the SLD optical feedback. S_1 and S_2 are the two interfaces of the duct where particles P1 and P2 are flowing. Lens L collimates the beam from the SLD and collect the back-reflected/scattered light.

on the reflectivity/diffusivity of the surfaces/particles. The returned optical power decreases rapidly as the number of reflections/transmissions increases [4] and away from the SLD. The higher contributions derive from the light back-reflected/diffused by the first interface S_1 and particles close to it. Neglecting homodyne effects between light back-diffused by the flowing particles, main interference effect derives from the optical beating between the light back-reflected by S_1 and the light back-diffused by the particles at a distance from S_1 shorter than the coherence length L_C of the emitted radiation. Similar situation happens at the second interface S_2 , however since the distance from the SLD is much larger, the amount of light back-reflected/diffused in the cavity can be neglected.

Considering only the particles that can generate interference phenomena with the light back-reflected by S_1 , i.e. $d < L_C$, and assuming the single scattering regime, the total light power diffused back to the SLD cavity is given by

$$P_d = I_i \cdot R(\lambda, \varphi) \cdot \Omega \cdot V_s \quad (1)$$

where:

- I_i is the illumination irradiance;
- $R(\lambda, \varphi)$ is the Rayleigh ratio of the particles sample that depends on the wavelength λ and scattering angle $\varphi = \pi$;
- $\Omega \approx \frac{\pi \cdot D^2}{4 \cdot d^2}$ is the observation solid angle. D is the diameter of the collimating lens L and d its distance from the duct (where $d \gg L_C$ has been supposed);
- $V_s \approx \pi \cdot \frac{L_C}{2} \cdot \left(\frac{D}{2}\right)^2$ is the scattering volume of interest assuming a beam size similar to the collimating lens diameter D .

Therefore S_1 and these particles act as an external mirror with equivalent reflectance:

$$R_{EXT} = R_S + (1 - R_S)^2 \cdot \frac{R(\lambda, \varphi) \cdot \Omega \cdot V_s}{\pi \cdot \left(\frac{D}{2}\right)^2} \quad (2)$$

$$R_{EXT} \approx R_S + \pi(1 - R_S)^2 \cdot R(\lambda, \varphi) \cdot \frac{L_C}{2} \cdot \left(\frac{D}{2d}\right)^2 \quad (3)$$

where R_S is the reflectance of surface S_1 .

Assuming R_{OUT} the reflectivity of the SLD emitting junction interface and $R_{eq} = \sqrt{R_{EXT} \cdot R_{OUT}}$, the power emitted by the SLD is [4]:

$$P_{SLD} = P_S \cdot \frac{\pi(1 - R_{eq})^2}{1 + R_S^2 \cdot G_S^2 - 2 \cdot R_{eq} \cdot G_S \cdot \cos(2 \cdot \beta \cdot l)} \quad (4)$$

where P_S is the guided power component of the spontaneous emission; G_S , β and l the single pass gain, the propagation constant and the length of the SLD cavity, respectively. Under the condition of weak feedback, the term $\sqrt{R_{OUT}} \cdot G_S$ multiplying the cosine function represents the optical amplification of the modulation index of interferometric signal due to the SM-SLD scheme. Typical values for G_S and R_{OUT} for commercial SLDs are 5000 and $1 \cdot 10^{-3}$ to $4 \cdot 10^{-3}$, respectively; thus, with respect to the standard Michelson interferometer the signal enhancement factor for the interferometric signal is on the order of $158 \div 316$.

B. Theoretical Doppler Spectrum

As shown in Fig.2, let's consider a single particle in a flowing fluid moving in a direction parallel to the duct axis at a distance r from the wall interface S_1 (i.e. interface tube material-flowing fluid).

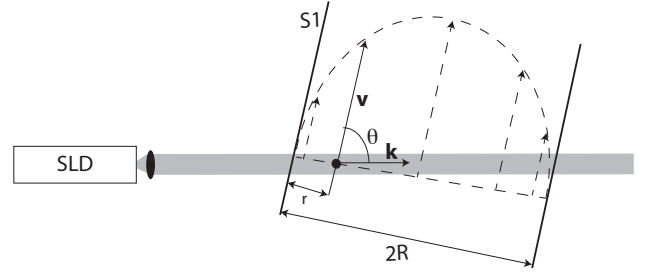


Fig. 2. The scattering particle flows along a streamline close to the duct wall S_1 with velocity v . The wavevector of the illumination light is k . We assume the laminar flow regime in the duct.

The optical path difference between the light back-reflected by S_1 and back-diffused by the particle is:

$$OPD = \frac{n \cdot r}{\sin \theta} \quad (5)$$

where n and θ are the refractive index of the flowing fluid and the Doppler angle respectively. Under the weak feedback condition, neglecting the DC terms and considering the effect on the beating signal of the SLD limited coherence, the detected optical power can be written as [5]:

$$P_{ac}(t, r) = 2 \left| \gamma_s \left(\frac{n \cdot r}{\sin \theta \cdot c} \right) \right| \cdot P_S \cdot G_S \cdot R_{eq} \cdot \cos(2 \cdot t \cdot \mathbf{v} \cdot \mathbf{k} + \varphi_0) \quad (6)$$

where γ_s is the SLD complex degree of coherence, \mathbf{k} is the wavevector, c is the speed of light in vacuum, \mathbf{v} is the velocity vector of the particle and φ_0 is the initial interferometric phase that will be omitted in the following discussion. The complex degree of coherence γ_s , given as the inverse Fourier transform of the spectral density of the emitted light, is expected to have a Gaussian shape [6]:

$$\left| \gamma_s \left(\frac{n \cdot r}{\sin \theta \cdot c} \right) \right| = \gamma_0 \cdot e^{-\left(\frac{n \cdot r}{\sin \theta} \right)^2 \cdot \frac{\ln 2}{L_C^2}} \quad (7)$$

Extending Eq. (6) to N identical particles acting as a continuum with linear density $\rho_X = N/2R$ over the duct diameter $2R$, the detected interferometric signal may be written as:

$$P_{ac}(t) = 2 \rho_x P_S G_S R_{EXT} \cdot \int_0^{2R} \left| \gamma_{sp} \left(\frac{n \cdot r}{\sin \theta \cdot c} \right) \right| \cdot \cos \left(4 \pi n \cdot \frac{v(r) \cos \theta}{\lambda_0} \cdot t \right) dr \quad (8)$$

Considering the laminar flow regime, all velocity vectors \mathbf{v} are aligned with the duct axis, and their modulus may be simply written as:

$$v(r) = v_0 \left(1 - \left(\frac{R-r}{R} \right)^2 \right) \quad (9)$$

where v_0 is the speed along the duct axis. Thus, if S is the flowing area of the duct section, the volumetric flow rate Q is:

$$Q \simeq \frac{1}{2} \cdot v_0 \cdot S \quad (10)$$

Since $\left| \gamma_{sp} \left(\frac{n \cdot r}{\sin \theta \cdot c} \right) \right|$ decreases rapidly as the value of r increases, the function $v(r)$ can be approximated with its first order Taylor polynomial:

$$v(r) \simeq 2 \cdot v_0 \cdot \frac{r}{R} \quad (11)$$

Therefore, in the laminar flow regime, the single particle at the position r moving along a streamline close to the internal duct's wall S_1 generates a Doppler frequency tone:

$$f_D(r) = 2 n \cdot \frac{v(r) \cos \theta}{\lambda_0} \simeq 4 n \cdot \frac{v_0 \cos \theta}{R \lambda_0} \cdot r \quad (12)$$

thus, the position r can be written as a function of the generated Doppler shift:

$$r(f_D) \simeq \frac{R \lambda_0}{4 n v_0 \cos \theta} \cdot f_D \quad (13)$$

As a result, changing the integration variable in Eq. (8) from r to $f = f_D$, the detected interferometric signal becomes equal to:

$$P_{ac}(t) \simeq \frac{\gamma_0 \rho_x P_0 G_S R_{EXT}}{2 n} \cdot \frac{R \lambda_0}{v_0 \cos \theta} \cdot 8 n \cdot \frac{v_0 \cos \theta}{R \lambda_0} \cdot \int_0^r e^{-\left(\frac{n R \lambda_0}{4 v_0 \cos \theta \sin \theta} \cdot f \right)^2 \frac{\ln 2}{L_C^2}} \cdot \cos(2 \pi f t) df \quad (14)$$

Such power arises from all the intensities scattered from any of the particles moving along the optical axis, weighted by the $|\gamma_S|$ function, whose spatial extent along the r direction is limited by L_C from the interface S_1 .

Concluding, the integral argument indicates that the spectrum of the monitoring photodiode photoelectric current is Gaussian:

$$I_{ac}(t) \simeq A \cdot e^{-\frac{f^2}{2 \cdot \sigma_f^2}} \quad (15)$$

where:

$$A = \eta \cdot \frac{\gamma_0 \rho_x P_0 G_S R_{EXT}}{2 n} \cdot \frac{R \lambda_0}{v_0 \cos \theta}, \quad (16)$$

$$\sigma_f = \frac{4 v_0 \cos \theta \sin \theta}{n R \lambda_0} \cdot \frac{L_c}{\sqrt{2 \ln 2}} = \frac{4 Q L_c}{n R S \lambda_0 \sqrt{\ln 4}} \cdot \sin(2 \theta) \quad (17)$$

and η is the monitoring photodiode responsivity.

III. EXPERIMENTAL SETUP

The activity objective is the measurement of the Doppler spectrum associated to a certain flow-rate through the hydraulic system, for a given set of scatterers concentrations. As shown in Fig. 3, this flow was finely controlled using a faucet with a multi-turn valve (MTV). The scattering fluid was a solution of water and Intralipid (Fat Emulsion, Fresenius Kaby) mixed in several concentrations, to evaluate the behavior of the system while changing the fluid optical characteristics.

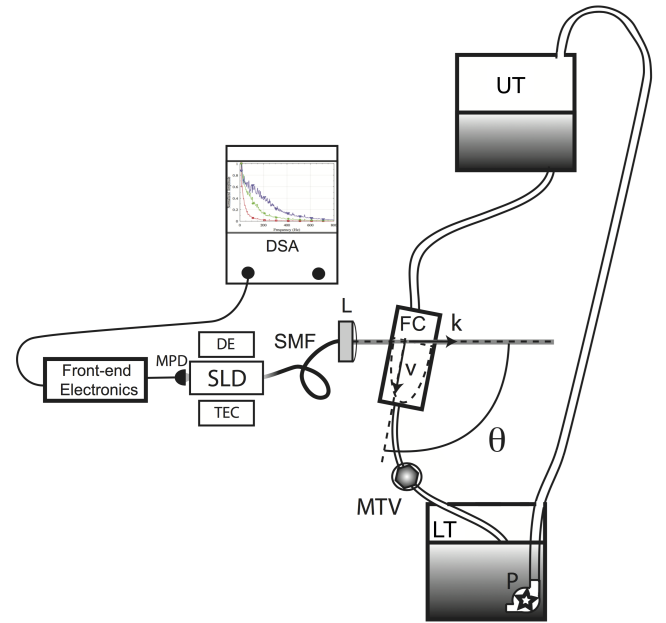


Fig. 3. Experimental setup: the scattering fluid flows through the cuvette, whose axis is tilted of an angle θ with respect to the optical one. Flow between the upper and lower tanks (UT and LT) is finely controlled using a faucet with a multi-turn valve (MTV). Scattered light is collected by the collimator L and a photocurrent is generated by the MPD. Custom front-end electronics handle the Doppler signal, that is then acquired by the DSA.

The optical system is based on a low cost superluminescent diode (SLD-381-MP-DBUT-SM-PD, Superlum). The SLD was controlled by using a thermoelectric temperature controller (TEC, model TED200C, Thorlabs) and fed by using a diode controller operating in constant current mode (DE, model LDC200C, Thorlabs). The SLD was powered with a constant current equal to 90.48 mA and the package temperature was kept at 25°C. In order to estimate the coherence length of the emitted radiation in water, according to Sheu and Luo [7], both the central wavelength λ_0 and the spectral

bandwidth $\Delta\lambda$ are needed: their nominal values are equal to 830 nm and 15 nm, respectively. It is known that a large variation of these two parameters can be observed from device to device, therefore a measurement of the optical spectrum was performed using an optical spectrum analyzer. The specifications provided by the manufacturer were confirmed by the measurements ($\lambda_0=833$ nm and $\Delta\lambda=15$ nm), thus the coherence length was calculated:

$$L_c = \frac{0.44 \cdot \lambda_0^2}{n \cdot \Delta\lambda} \approx 15.3 \mu\text{m} \quad (18)$$

The light beam generated by the SLD is guided through a single mode optical fiber (SMF), which is connected to a non contact-receptacle style collimator (HPUCO-23-850-S-2.7AS, OZ Optics). This fiber collimator has an aspheric lens with focal length of 2.7 mm and a central wavelength of 850 nm. The cuvette was mounted on a XYZ stage in order to allow the user to align the system, as well as to change the Doppler angle when needed (Fig. 4). This tilt regulation is fundamental to allow both the light reflected by the inner wall S_1 of the cuvette and the light scattered by the particles in its proximity (within $L_C/2$) to be collected by the collimator and then guided through the fiber to the MPD, as shown in Fig.2.

The current photogenerated by the monitor photodiode was processed by a custom made front-end electronic circuit and then acquired by the digital spectrum analyzer (DSA, SR785-Stanford Research). The scattered light collected when the fluid was filling the cuvette but not flowing through it, generated a photocurrent equal to 203 μA , whereas fluctuations related to Doppler signal are 5 orders of magnitude smaller. Hence it was important to remove this DC current in order to perform a suitable amplification of the AC signal components by a transimpedance amplifier. A current sink was realized by using a 2N2222 BJT with emitter degeneration to reduce its temperature sensitivity and allow finer tuning of the sink current by means of a variable resistor. Simulations showed that in this configuration the BJT current could vary from 175 μA to 255 μA . The photogenerated current may change as a result of a variation of the Doppler angle or to modifications of the fluid optical parameters (such as absorption or diffusivity).

The hydraulic system consisted in an upper tank (UT), filled with 12 liters of water and a lower tank (LT) to collect the fluid flowing through the system. The flow was regulated by mean of a multi-turn valve (MTV): a pump (P) was placed in the LT to maintain the water level in UT almost constant. Using this system, the flows were changed from 1.1 cm^3/s to 15 cm^3/s , while Intralipid was mixed with distilled water at increasing concentrations, from 0.015% to 0.36%. To confirm the laminar flow hypothesis, the Reynolds number was calculated. Since the cuvette has a square cross section, the hydraulic diameter is going to be equal to the side dimension ($R=1$ cm). Thus, for the highest flow rate considered (15 cm^3/s) we obtained a Reynolds number of 73.5, which is well below the threshold value for turbulence (4000) [8, 9].

IV. EXPERIMENTAL RESULTS AND DISCUSSION

The Doppler spectra were acquired at different flow-rates, varying from 1.1 cm^3/s to 15.0 cm^3/s , and scattering particles

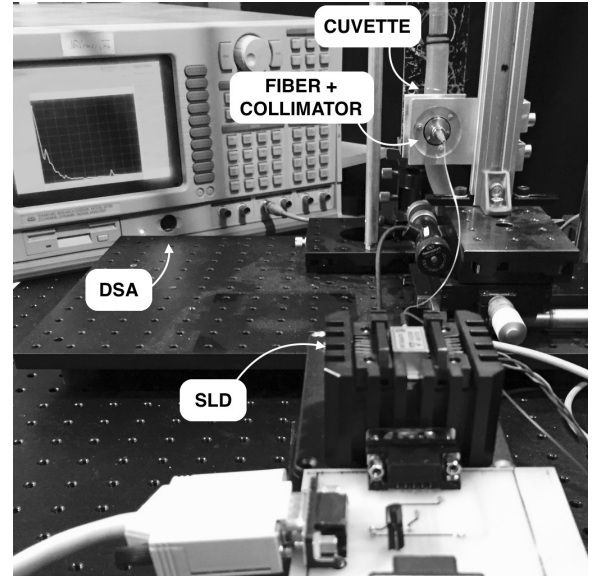


Fig. 4. Picture of the experimental setup. DSA is the digital signal analyzer, SLD is the superluminescent diode.

concentrations. A higher flow-rate means a greater speed of the scattering particles along the cuvette, hence a broader Doppler spectrum is expected according to Eq.(12). Different scattering particles concentrations were obtained by preparing solutions of Intralipid in water, which concentrations were ranging from 0.015 % to 0.36 %.

The signal amplified by the front-end electronics was acquired using the DSA. For each concentration and flow, three signal acquisitions were performed. Moreover, every single acquisition is the result of 50 acquisitions that are automatically averaged by the DSA.

A. System calibration, uncertainty and Doppler angle determination

To determine the doppler angle θ , the system was calibrated. We acquired 20 Doppler spectra for each of the three reference flow-rates ($Q_1=2.1 \text{ cm}^3/\text{s}$, $Q_2=7.5 \text{ cm}^3/\text{s}$ and $Q_3=15 \text{ cm}^3/\text{s}$). Reference values for Q_1 , Q_2 and Q_3 were determined by measuring the time needed to fill a graduated beaker up to a fixed volume. The flowing solution had an Intralipid concentration equal to 0.06% during the calibration. According to our theoretical model, the higher the flow-rate the broader is the Doppler power spectral density (PSD). Each of the 60 acquired PSDs was fitted by a Gaussian function to calculate the best gaussian amplitude and variance that minimize the mean squared errors. As an example, Fig. 5 shows the experimental data acquired at Q_3 and the corresponding best fit. The average normalized PSDs and their Gaussian fits for each of the three flow-rates are shown Fig. 6.

For each of the three flow-rates, the average σ and its standard deviation were calculated over the 20 acquired spectra. Fig. 7 shows the resulting values as a function of the flow-rate. Error bars show as the standard deviation increases linearly with the flow-rate. As predicted by our theoretical model, when the flow increases the frequency components

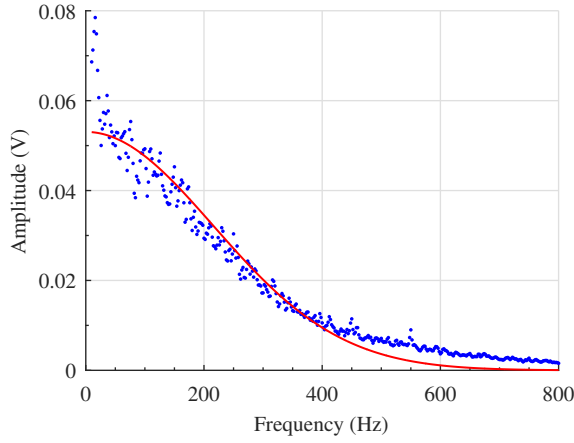


Fig. 5. Gaussian fit (bold curve) example of an acquired PSD, referred to a fluid flow rate equal to Q_3 with an Intralipid concentration of 0.06%. The calculated value of σ is 306.1 Hz, and the goodness of fit, R^2 , is 96%.

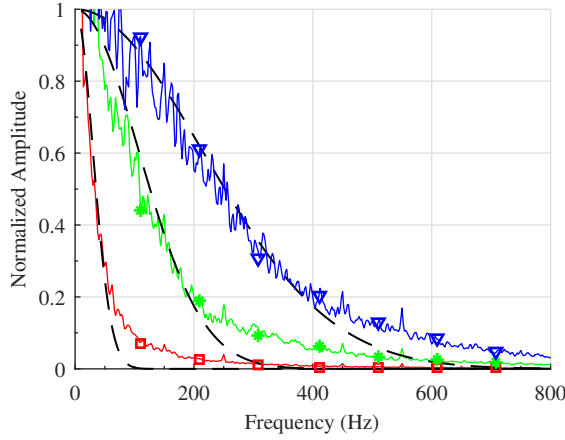


Fig. 6. Averaged normalized power spectral densities, acquired at the flow-rates Q_1 (squares \square), Q_2 (asterisks $*$) and Q_3 (triangles \triangle). Dashed curves represent the best Gaussian fit.

become weaker since the signal power is spread over a broader spectrum. Therefore signal-to-noise ratio decreases at high flows, hence leading to a greater uncertainty when computing σ . The slope of the linear interpolation shown in Fig. 7 represents the sensitivity of the system with an Intralipid concentration of 0.06%. The best linear fit provides a slope equal to 20.2 cm^{-3} .

According to Eq. (17), the value of the Doppler angle theta can be calculated as:

$$\theta = \frac{1}{2} \cdot \arcsin\left(\frac{m_{cal} n R^3 \lambda_0 \sqrt{\ln 4}}{4 L_C}\right) \quad (19)$$

where m_{cal} is the calibration curve's slope at the reference concentration. The calculation returns 6.19° as result.

B. System Linearity and measurement error

System linearity was verified by acquiring the Doppler spectra for ten different flow-rates ranging from $1.1 \text{ cm}^3/\text{s}$ to $15 \text{ cm}^3/\text{s}$. The Intralipid concentration was kept constant to 0.06% for all the measurements. The measurement procedure

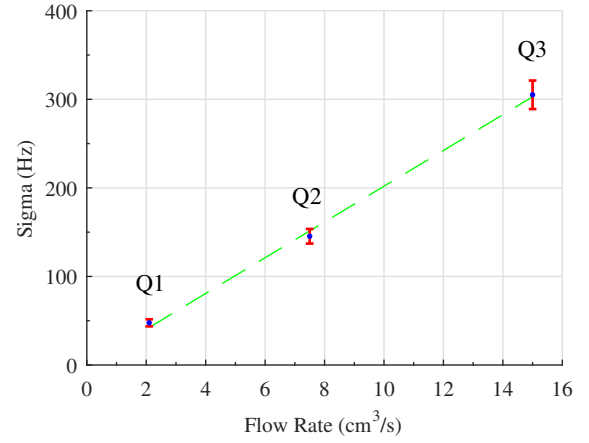


Fig. 7. Calibration at the reference Intralipid concentration of 0.06%. For each flow, the average value of σ is represented with a dot (\bullet) and the standard deviation with an error bar (I). The linear interpolation dashed line has a goodness of fit equal to 99.79%. Standard deviation values are 4.0 Hz, 8.2 Hz and 16.1 Hz for Q_1 , Q_2 and Q_3 , respectively

consisted in the acquisition of three PSDs for each flow-rate (each obtained as the average of 50 acquisitions), then the average spectrum for each flow-rate was calculated as the average of these three PSDs. By performing the best Gaussian fit of each averaged spectrum, the value of σ was computed for every flow-rate. Then, by using the calibration constant obtained in the previous section, the estimated flow-rate was calculated. The comparison between reference flows and estimated flows is shown in Fig. 8. Linear interpolation of the experimental data (bold line) exhibits a slope of 1.088 and a Pearson coefficient of about 99%. Fig. 9 shows the absolute error as function of the reference flow-rate. The measurement absolute error in the range $1.1 \text{ cm}^3/\text{s}$ to $15 \text{ cm}^3/\text{s}$ is, in modulus, less than $0.8 \text{ cm}^3/\text{s}$.

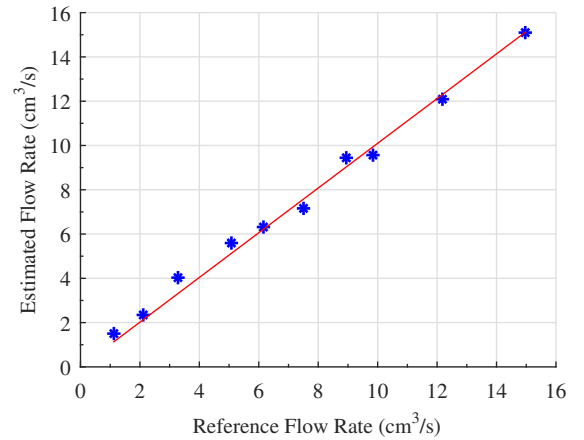


Fig. 8. Estimated flow-rates with respect to the reference ones. The bold line is the linear interpolation of the experimental data.

C. Effects of the multiple scattering on the system sensitivity

According to our theoretical model, system sensitivity shouldn't be dependent on the scatterers concentration. However, while increasing scattering particles concentration, multiple scattering can occur. Since photons walk between scatterers

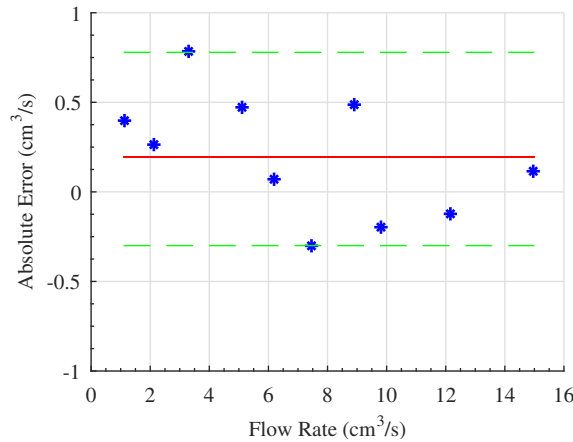


Fig. 9. Absolute measuring error as a function of the reference flow-rate. Dashed lines represent the maximum and minimum error, while the bold line is the average error value.

is random, the Doppler contribution of the single particles becomes non-predictable thus increasing the noise and reducing the useful signal. As an example, Fig.10 shows three different spectra acquired at the same flow-rate but at different intralipid concentrations, i.e. $C_1=0.06\%$, $C_2=0.12\%$ and $C_3=0.36\%$. Note as, increasing the scatterers concentration the high frequency components of the acquired spectrum tend to disappear, thus collapsing the spectra obtained at different flows in the low frequency region by reducing the possibility to discriminate them. Basically this results in a reduction of the system sensitivity.

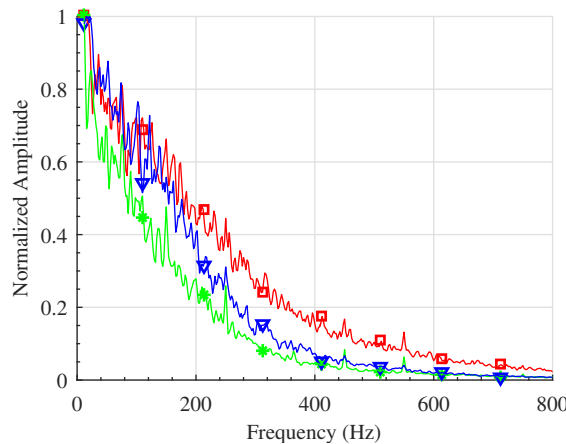


Fig. 10. Three normalized PSDs obtained at three different Intralipid concentrations ($C_1 < C_2 < C_3$). In particular, the red curve (\square) is for C_1 , the blue one (∇) is for C_2 and the green one ($*$) is for C_3

To verify the robustness of our system to this effect, the system sensitivity has been measured at six different Intralipid concentrations from 0.015% to 0.36%. Measurements at even higher concentrations are possible, however the performance of our front-end electronics could not assure a suitable signal-to-noise ratio. Calibration curves were calculated as described in section IIIA for all of the six Intralipid concentrations and the corresponding sensitivities have been calculated.

Tab. I reports the sensitivities of the measuring system with

respect to the Intralipid concentration. After increasing at very low scatterers concentrations, the sensitivity decreases of about 32% in the considered range of Intralipid concentration. This trend confirms our prediction and is consistent with possible occurrence of multiple scattering.

TABLE I
SYSTEM SENSITIVITY AS A FUNCTION OF THE INTRALIPID CONCENTRATION

Concentration (%)	Sensitivity ($1/\text{cm}^3$)
0.015	18.02
0.03	18.48
0.06	20.19
0.12	15.02
0.24	13.94
0.36	13.86

V. CONCLUSION

To perform flow measurements, SM-SLD can be implemented using a pigtail device with a simple design in which the reference arms is defined by the inner interface of the duct. The advantages of this common-path geometry include greater ease of alignment, reduced sensitivity to vibration and greater stability. Low-coherence approach allows considering effortlessly a small well-defined scattering volume thus reducing the probability of multiple scattering. Future developments include the exploration of the system behavior at higher flow-rates, up to the lower bound where turbulent flow begins to occur. In addition, to test the system at higher scatterers concentrations an improved electronic circuit with a better noise performance is under development.

REFERENCES

- [1] G. Giuliani, M. Norgia, S. Donati, and T. Bosch, "Laser diode self-mixing technique for sensing applications," *Journal of Optics A: Pure and Applied Optics*, vol. 4, no. 6, p. S283, 2002. [Online]. Available: <http://stacks.iop.org/1464-4258/4/i=6/a=371>
- [2] S. Donati, "Developing self-mixing interferometry for instrumentation and measurements," *Laser and Photonics Reviews*, vol. 6, no. 3, pp. 393–417, 2012. [Online]. Available: <http://dx.doi.org/10.1002/lpor.201100002>
- [3] S. Donati and M. Norgia, "Self-mixing interferometry for biomedical signals sensing," *IEEE Journal of Selected Topics in Quantum Electronics*, vol. 20, no. 2, pp. 104–111, March 2014.
- [4] L. Rovati, L. Pollonini, and F. Docchio, "A system for the inspection and quality control of glass slabs," *Review of Scientific Instruments*, vol. 73, no. 9, pp. 3386–3391, 2002. [Online]. Available: <http://dx.doi.org/10.1063/1.1497501>
- [5] L. Rovati, S. Cattini, and N. Palanisamy, "Measurement of the fluid-velocity profile using a self-mixing superluminescent diode," *Measurement Science and Technology*, vol. 22, no. 2, p. 025402, 2011. [Online]. Available: <http://stacks.iop.org/0957-0233/22/i=2/a=025402>
- [6] M. Born and E. Wolf, *Principles of Optics*, 7th ed. Cambridge University Press, 1999.

- [7] F.-W. Sheu and P.-L. Luo, "Temporal coherence characteristics of a superluminescent diode system with an optical feedback mechanism," in *Education and Training in Optics and Photonics*. Optical Society of America, 2007, p. EMB6. [Online]. Available: <http://www.osapublishing.org/abstract.cfm?URI=ETOP-2007-EMB6>
- [8] *Fluid Mechanics: An Introduction to the Theory of Fluid Flows*. Berlin, Heidelberg: Springer Berlin Heidelberg, 2008, ch. Unstable Flows and Laminar-Turbulent Transition, pp. 495–522.
- [9] S. Gavrilakis, "Numerical simulation of low-reynolds-number turbulent flow through a straight square duct," *Journal of Fluid Mechanics*, vol. 244, pp. 101–129, 11 1992.

Luca Di Cecilia received the M.S. degree (magna cum Laude) in electronic engineering from the University of Modena and Reggio Emilia (Modena, Italy) in 2015, where he is currently enrolled at the Ph.D. School in ICT. His research focuses on optoelectronic instrumentation and measurements in the biomedical field.

Stefano Cattini (M'09) was born in Sassuolo, Italy, on December 21, 1980. He received the Engineering degree in electronic engineering (Honours) and the Ph.D. degree in Electronics and telecommunications from the University of Modena and Reggio Emilia, Modena, Italy, in 2005 and 2009, respectively. Since 2005, he has been with the University of Modena and Reggio Emilia, Modena, Italy, where he has held lecturing positions and he is currently a researcher. From 2015 he is also a researcher at the Science and Technology Park for Medicine, Mirandola, Italy. His research interests cover the design and validation of new measurement methods and measuring systems.

Fabio Giovanardi received the M.S. degree in electronic engineering from the University of Modena and Reggio Emilia, Modena, Italy, in 2015. He is currently working as an Engineer within the R&D Department at MD Microdetectors (Modena, Italy), where he is studying and developing new electromagnetic sensors.

Luigi Rovati (M'92) received his first-class honours degree in Electronic Engineering in 1989 and PhD in Electronic Engineering and computer science in 1994 both at the University of Pavia, Italy. From 1995-2001 he was researcher and Assistant Professor at the Department of Electronics for the Automation at the University of Brescia. He joined the Department of Information Engineering at the University of Modena and Reggio Emilia, in 2001, where he presently is Associate Professor of Electronic Instrumentation and Measurement Science (ING-INF/07). His research activities have been towards the study and the development of low-noise, high- performance, innovative instrumentations. The present involvement of his research activity is related to the design of innovative biomedical instrumentation mainly oriented to ophthalmic diagnostic systems. The published papers production (more than 150 publications) testifies the level of the developed activity . Dr. Luigi Rovati was involved in various research projects between University and industrial partners.